3

The Effects of Sintering Temperature Variations on Microstructure Changes of LTCC Substrate

Rosidah Alias
TM Research & Development Sdn. Bhd.
Malaysia

1. Introduction

The successful development and commercialization of high performance ceramic materials has attracted much attention especially for multilayer substrates using the Low Temperature Co-fired Ceramic (LTCC) technology. This technology has become a popular technology for automobiles and wireless communications due to the advantages of the excellent combination of electrical, thermal, mechanical and chemical stability for a wide range of applications, thus allowing preparation of 3-dimensional circuits incorporating passive components within a multilayer construction (Matters-Kammerer et al., 2006; Zhou et al., 2008). This approach also allows the presence a number of interfaces and thus reduction of the overall substrate size and cost can be realized (Lo and Duh, 2002; Chen et al., 2004 and Zhu et al., 2007). The circuits are capable of withstanding sintering during processing temperatures up to 1000 °C. For telecommunication applications the usage of ceramic is implemented in Telecom control station and power supply circuits for the capability to dissipate excess heat and maintain dimensional control stability of the ceramic package. This is important where back-up power is required to maintain operation during primary power outages when cooling is restricted (Barlow and Elshabini, 2007). Another important parameter for wireless communication devices is the requirement to have low dielectric loss (tan $\delta \sim 10^{-3}$ or less) for higher processing speed, higher dielectric constant ($\varepsilon' > 10$) for miniaturization of the devices and higher integration density (≥ 3 g/cm^3) (Kume et al., 2007; Long et al., 2009). For this reason, it is important to prepare high quality LTCC substrate/package whose properties are strongly dependent on microstructure, phase purity and sintering temperature (Xiang et al., 2002). Therefore the microstructure must be carefully controlled to get dense and fine grained ceramics in order to improve their properties and reliability in many applications (Hsu et al., 2003).

The starting point of the LTCC technology is the development of LTCC tape materials containing a glass-ceramic system that usually needs to show good compatibility with the paste system which acts as a conductive track for RF signal transportation from one location on the circuit to another. It should also have low energy loss in microwave applications to make sure high circuit performance can be achieved (Wang et al., 2009). One of the most important processes in LTCC manufacturing of multilayer LTCC substrates involves co-

firing of metal and glass-ceramic. The main problem in the development of materials for LTCC integrated modules arises from the chemical incompatibility of the different materials within the module during the sintering process (Valant and Suvorov, 2000). So, mismatch in sintering kinetics, sintering stress, density variations between tape layers and non-uniform shrinkage of the individual tapes should be taken into consideration to avoid some defects such as delamination, blister, and camber form during a multilayer LTCC process. Therefore, the processes that result in the above mentioned defects must be completely understood before the processing parameters and material compositions are optimized.

Thick-film technology is a method whereby conductive, resistive and dielectric pastes are applied to a ceramic substrate. There are various available ways of producing thick-films such as dip coating, spin coating, screen printing and chemical vapor deposition technique down to 25 μm thickness. However the screen printing method is simpler, more convenient and the most cost effective method to transfer the desired thick-film pattern onto the substrate in order to realize interconnect films with a thickness ranging from 3-15 μm which depends upon the screen printing parameter. Highly conductive metals such as copper, silver and gold are typical electrode materials in LTCC components and modules. A silver (Ag) conductor is very attractive because the price of silver is much cheaper than that of others and can be fired in air. It also has some advantages such superior electrical conductivity and good thermodynamic stability below 200 °C. Above 200 °C it deoxidize to metallic silver (Imanaka, 2005; Bangali et al., 2008; Jean et al., 2004). For the LTCC process the dielectric ceramics and silver should be cofired simultaneously so it is important to carried out the sintering process below the melting point of the metal electrode such as Ag (961 °C) to reduce sintering mismatch between each other which form some defects for the whole substrate (Feteira and Sinclair, 2008; Chang and Jean, 1998; Long et al., 2009). With regard to the co-firing process technology and to get detailed understanding of LTCC process behavior, the mechanism of low temperature sintering was studied by Valant et al., in 2006 using $BaTiO_3$ whose original sintering temperature was about 1250 °C -1300 °C. They used a small amount of Li_2O as a sintering aid and found that small amount of sintering aid about 0.3 wt% was able to reduce the sintering temperature to 820 °C and ceramics with more than 95% of relative density could be produced.

The study of transition metal elements especially controlling the properties of silver is of great importance from the view point of industrial applications. It is not a simple task and demands thorough understanding of structure ⇔ property ⇔ processing relationship (Despande et al., 2005). The overall behavior of silver metal is influenced by the nature of atoms, the size of the grain and the nature of grain boundaries in addition to controlled chemical composition and preparation conditions. So the material specifications/characteristics of the thick-film can fulfill conductor paste requirements in a wide range of applications. Typically, a thick-film conductor paste consists of metal powder as a major component and glass and/or oxide (minor) dispersed in an organic medium (Sergent and Harper, 1995). The metal powder forms a continuous film on the substrate upon firing. The role of the glass and /or oxide in the conductor paste is to help the metal film adhere to the substrate. The investigation of the preparation of LTCC packages using glass + ceramic and glass ceramic system with high electrical conductivity such as gold and silver has been conducted by several researchers such as Shimada et al., 1983, Tummala, 1991, Imanaka and Kamehara, 1992, Jean et al., 2001 and Bangali et al.,

2008. Most of their studies have been performed on multiphase material systems and focused crystallization behavior of the systems. Wang and Zhou (2003) have studied the relation of densification and dielectric properties of glass ceramics with different compositions selected from the CaO-B_2O_3-SiO_2 system. They have found that too high sintering temperature will ruin the properties and sintering with a heating speed of 10 °Cmin^{-1} at 850 °C for 60 min is an optimal technology for CBS system. They also notice that too much B_2O_3 will damage the dielectric properties of the glass ceramics (Wang and Zhou, 2003). More recently, Hsi and co-workers have further studied the relation of silver and LTCC. They demonstrate the easy method to decrease effectively the diffusivity of silver ions in LTCC dielectrics by adding 5 wt % of SiO_2 (Hsi et al., 2011). However, not much literature has been found to investigate the microstructure changes of silver conductor and glass-ceramic substrate by changing the sintering temperature and this situation may not be very helpful in understanding the surface properties of the printed conductor and the microstructure of glass-ceramic system in this project. Nevertheless, the results obtained in this work can provide useful findings for researchers and industries.

There are a few factors that determine the microstructure for both printed conductor and LTCC substrate such as the quality of the raw materials and the sintering temperature. The parameters of microstructure are the grain size, grain size distribution, pore size and pore size distribution and the density. The size, shape and also the distribution of grain size and pore size of the conductor and glass-ceramics will vary with preparation conditions and techniques. The objective of this work is to investigate the effect of sintering temperature variations on the microstructure of both metal and ceramic materials of the LTCC substrate for microwave applications.

In this chapter, the work is constructed as follows; firstly, a simple transmission line pattern on the eight layers substrate is fabricated using a standard LTCC technology. Printed patterns were dried in a box oven for 10 minutes at about 70 °C to remove the organic solvent slowly before cofiring process in order to avoid blister, void formation, delamination, cracks and camber effect. These undesirable defects are usually formed due to the different shrinkage rates of LTCC tape and thick-film paste during firing (Hsueh and Evans, 1985; Hrovat et al., 2009). The film was then fired at various sintering temperatures of 800 °C to 900 °C at 25 °C increments. Generally at peak firing temperature the film achieves desired electrical properties and the ceramic composite also has undergone changes in physical properties. Further, sample characterizations were done such as crystal structure determination, linear shrinkage, density measurement and microstructure observation for both metal and LTCC substrate. After that sample analysis and detail discussion is carried out to explain the research findings.

2. Experimental procedure

In the following sections, the various process stages will be described. The effect of process variables on the physical properties and microstructure of the finished product has always been a subject of great importance. The factors that have the most influence on these properties are the purity of the constituent oxides, their proportions and homogeneity in the powder mix and the control of temperature and atmosphere during sintering.

The key stages in the fabrication of glass-ceramics are sintering process of various components together. During these processes the constituent atoms redistribute themselves in such a way as to minimize the free energy of the system. This involves a considerable movement of ions, their inter-diffusion to form a new phase, the minimization of the internal surface area and increase in grain size.

2.1 LTCC multilayer substrate preparation

In the present work, the commercial Ferro A6S was chosen and cut into 8 pieces for the required dimension (21 mm x 21 mm) using a die cutting machine (ATOM SE 20C). The multilayer stack was prepared by standard LTCC process flow as shown in Fig. 1. The thickness of the green tape is about 100 µm for each layer; the green tape was punched and screen printed with CN 33-391 for the surface and inner conductor and CN 33-407 for via fill. The printed pattern was then stacked using a manual stacker plate. The stacked substrate was then laminated by using an isostatic laminator system under pressure and temperature of 3000 psi (21 MPa) and 70 °C respectively to ensure that the layers of the stack are well adhered to each other and to form a compact multilayer substrate. The laminated substrate was placed in a tube furnace and fired using a sintering profile as suggested by the tape manufacturer. The substrates were sintered in the temperature range of 800 °C to 900 °C at 25 °C increments. This sintering is the most critical process step because during the firing step the material becomes a compact ceramic LTCC substrate and its properties are determined. Through sintering, a transformation from the original porous compact to a dense ceramic takes place (Kingery, 1976). At a high temperature, the particles are in an increased contact and the particles grow together to form crystallite grains.

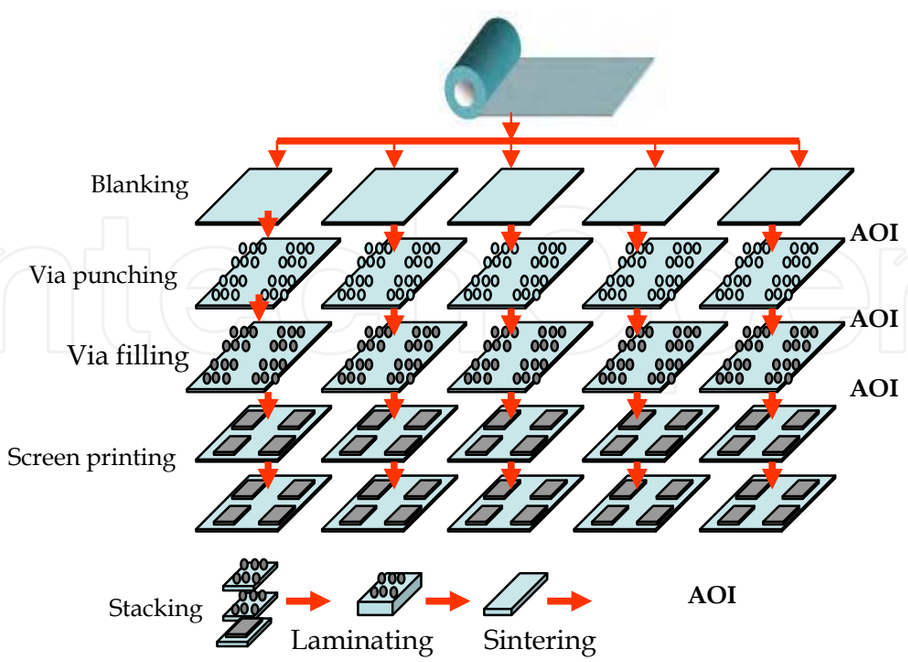

Fig. 1. LTCC Multilayer Fabrication Process Flow.

A typical practice is to heat up the furnace to 450 °C with a gradient of about 2-5 °C/min for 1 hour to completely remove the organic solvent. In the next 2 hours the temperature is raised to about 850 °C at which the sintering process of the composite material is started. The temperature remains constant for 10 minutes to finish the sintering. The last stage is the cooling period which takes about 3 hours depending on the size of the product. This firing condition is selected because of the practical experience on thick-film circuit and suggested by the tape manufacturer.

2.2 Substrate characterizations

2.2.1 Crystal structure determination

The structural characteristics of the LTCC material and metal surface were measured using a Pan Analytical Diffractometer system operating at 45 kV and 40 mA and employing CuK_{α} radiation with $\lambda = 1.54060$ Å. The scanning measurements were 2θ in a range from 2° to 80°, in steps of 0.05° of 2θ and a counting time of 25 s per step. The average crystallite size of all the samples is determined from the full width at half maximum (FWHM) of the (1 1 1) reflection peak in the XRD patterns by using the Debye Scherrer formula shown in equation (1), (Klug & Alexander, 1974).

$$D = \frac{0.94\lambda}{\beta\cos\theta} \tag{1}$$

where λ is the wavelength of the incident x-ray; β is the full width at half maxima; θ is the Bragg's diffraction angle.

2.2.2 Shrinkage

The most important point to bear in mind in the sintering process is controlling the variation in dimensional changes. One of the methods to control the dimensional changes in terms of shrinkage is through the control part as shown in Fig. 2. The steps are as follows:

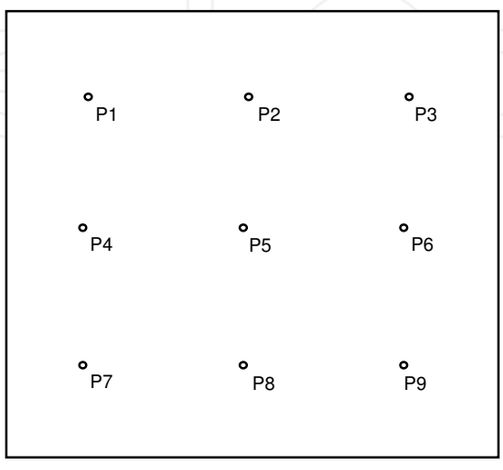

Fig. 2. Control part (Ferro).

1. The control part study main point is to study shrinkage variation. Measurements are taken before and after firing. Measure thickness (Z) of each laminate midway between each via and record data. There will be eight (8) measurements total. Next, measure the average width and length of each laminate by measuring from corner to adjacent corner and record data.
2. Next, measure the distance between each via. Record data, there are 12 measurements needed. Via holes 1,2 - 2,3 - 4,5 - 5,6 - 7,8 - 8,9 are for the X direction. Via holes 1,4 - 2,5 - 3,6 - 4,7 - 5,8 - 6,9 are for the Y direction.
3. The shrinkage and density of sample test pattern are calculated using equation (2).

$$\text{Shrinkage} = \left(\frac{\text{Length}_{\text{before fired}} - \text{Length}_{\text{after fired}}}{\text{Length}_{\text{before fired}}} \right) \text{x}100\% \quad (2)$$

For the substrate, linear shrinkage was measured along the compaction direction and the diametrical shrinkage from the geometry of the substrate. Repeatability and consistency of the shrinkage percentage must be the top criteria when designing the LTCC product because the shrinkage of LTCC substrate depends on the reactivity of the co-fired material containing ceramic oxide, glass, metal, organic solvent and also the firing conditions such as temperature, time and ambient air. Better reproducibility increases the uniformity of finished product characteristics and therefore increases the process yield. It is not an easy task because all process parameters (lamination, binder burnout, sintering) and material properties (high temperature reactivity, thermal expansion, etc.) must be matched (Rabe et al., 2005). Furthermore, the material quality of the finished product and process conditions also must be optimized in micro and macro structures in order to make sure work in progress are homogeneous at each process step (Imanaka, 2005). In order to achieve desired shrinkage data, the process engineer must establish control of the critical process variable. In commercial production, the designed shrinkage is generally between 12-16 % for XY direction and 20-25 % for Z direction.

2.2.3 Microstructure observation

The surface morphology and composition of the LTCC material and the printed material were observed by using a FEI NOVA Nano SEM 230 machine equipped with an Energy Dispersive X-ray (EDX) detector to reveal the microstructure of the resulting product. Most of the samples were imaged several times, with at least three pictures in each case from different areas of the sample. The thickness and width of conductive traces were measured by an optical microscope and SEM through the cross section view respectively. The average grain size was calculated using the line intercept method. The EDX spectrum is used to identify elements within a sample.

2.2.4 Density measurement

The properties of the final ceramic composite materials depend on the sintered density of the whole substrate. A stacked and laminated LTCC substrate before firing consists of a relatively porous compact of oxides in combination with a polymer solvent. During

sintering the organic solvent evaporates and the oxides react to form crystallites, or grains of the required composition, the grains nucleating at discrete centers and growing outwards until the boundaries meet those of the neighboring crystallites. During this process, the density of the material rises; if this process were to yield perfect crystals meeting at perfect boundaries the density would rise to the theoretical maximum, i.e. the x-ray density, which is the material mass in a perfect unit crystal cell divided by the cell volume. In practice imperfections occur and the sintered mass has microscopic voids both within the grains and at the grain boundaries. The resulting density is referred to as the sintered density. The density of the sample was measured using the Archimedes principle shown in equation (3);

$$\rho = \left(\frac{W_a}{W_w} \right) \rho^* w \tag{3}$$

where W_a = weight of sample in air
W_w = weight of sample in water
ρ^*_w = density of water = 1 gcm^{-3}

The percentage theoretical density ($\%D_{th}$) was calculated using this formula:

$$\%D_{th} = (\text{measure density} / \text{theoretical density}) \times 100\% \tag{4}$$

The theoretical density of Calcium Boron silicate ($CaB_2Si_2O_8$) was calculated using equation below:

$$\rho = \frac{N_C A}{V_C N_A} \tag{5}$$

Where N_C = No. of molecules per unit cell, A = molecular weight, V_C = volume of one molecules and N_A = Avogadro number. So the theoretical density of $CaB_2Si_2O_8$ was calculated by taking the molecular weight of $CaB_2Si_2O_8$ to be 245.87g. Since orthorhombic structure of $CaB_2Si_2O_8$ have four formula units per unit cell, the molecular weight of one cell is (4) x (245.87) = 983.48. The volume of the orthorhombic structure unit cell is *a* x *b* x *c*. The volume of a mole of the material is therefore N_A x a x b x c, where N_A is Avogadro's number. The unit cell edge *a, b and c* (Å) of $CaB_2Si_2O_8$ = 8.7500, 8.0100 and 7.7200 therefore *a* x *b* x c = 541.08 $Å^3$. As $1Å^3 = 10^{-24}cm^3$, A x *a* x *b* x *c* is therefore:

$$[6.023 \times 10^{23}][541.08 \times 10^{-24}] = 325.92 \text{ cm}^3$$

so, theoretical density is mass/volume equals to 983.48 g /325.89 = 3.018 g/cm^3.

The theoretical density ρ_x was calculated as above. The percentage of porosity of the sample was calculated using the relation as below:

$$P = 1 - \frac{\rho}{\rho x} \tag{6}$$

where ρ is the measured density of the sample.

3. Results and discussion

3.1 Phase analysis

Results of the crystallization behaviour of glass-ceramic Ferro A6S substrate sintered at various sintering temperatures are presented in Fig. 3. It can be seen that the small intensity peaks which appeared for the 800 °C sintering belongs to crystalline phases of Calcium Silicates with various stoichiometric ratios Ca_2SiO_4, and Ca_3SiO_5. Increasing the temperature to 825 °C and 850 °C, the two phases of Calcium silicate phase are still maintained but accompanied by a new phase of Calcium Borate (CaB_2O_4). As the sintering temperature increases the formation of Danburite ($CaB_2Si_2O_8$) start to appear in small intensities while crystalline phases of Ca_2SiO_4, Ca_3SiO_5 including $CaSiO_3$ and CaB_2O_4 phase are maintain in this composite system. They are the stable phases when crystallization is complete. Due to the high peak intensity of $CaSiO_3$ at $2\theta \approx 29.9572$, it can be noted that the main phase in this system is Calcium Silicate $CaSiO_3$. The above results were consistent with the work done by Chang and Jean (1999). However, from their studies, they concluded that no crystalline phase was detected at temperatures below 850 °C. The crystallite size as a function of sintering temperature was calculated from the most intense peak (3 1 1) by using the Scherrer equation (equation 1) and tabulated in Table 1.

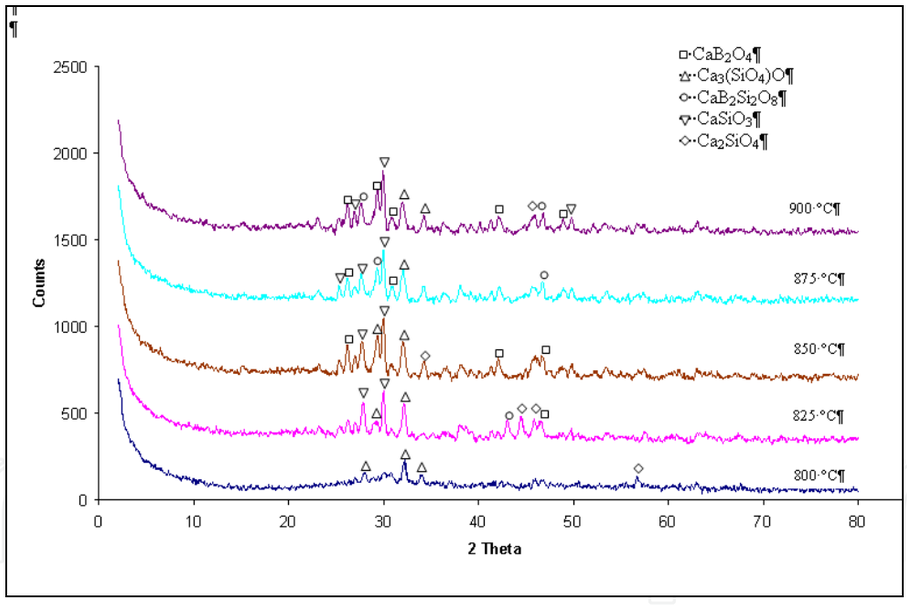

Fig. 3. XRD pattern of the LTCC substrate sintered at various sintering temperature.

Generally sintering temperature plays an important role in determining the crystallite size of the silver paste. However the range of sintering temperature 800 °C and 825 °C in this study did not play an important role in the variation of the crystallite size evolution due to the stable growth of the grains. However, increasing sintering temperature slightly variation of crystallite size was obtained. Thus a further investigation of sintering temperature whether increase or decrease is necessary in order to see the significance different of the crystallite size.

Sintering Temperature (°C)	2 Theta	$D_{spacing}$	Crystallite size (D_p)
800	32.2207	2.77597	29.2565
825	32.1571	2.78132	29.2518
850	32.0970	2.78638	19.4982
875	32.0726	2.78845	25.0677
900	31.9778	2.7965	17.5432

Table 1. Parameter of XRD.

3.2 Physical measurements

3.2.1 Density

The physical data of the LTCC substrate fired at various temperatures are tabulated in Table 2. The relationship of density with sintering temperatures is shown by Fig. 4. The results reveal decreasing trend of the density with sintering temperature with the highest density being 2.992 g/cm^3 at 800 °C and the lowest density is 2.806 g/cm^3 at 900 °C. The densities of all the samples were between 92 to 99 % of theoretical density (3.018 g/cm^3). This trend seems to contradict the normal expected phenomenon that increasing sintering temperature should increase the density. As is well known the sintering process of a ceramic based material is the sintering of the powder compact into the final material. During this step, the porosity decreases and the microstructure of the material develop; this determines its final performance. During the sintering of a homogeneous material the porosity induced during the preparation of the green compact gradually decreases, depending on the powder morphology, agglomeration, the presence of liquid phase sintering and the sintering condition itself. However, the sintering of heterogeneous materials in the LTCC substrate, reactive sintering occurs in the concurrent process of reaction and densification during sintering. A variety of reactions are possible: oxidation-reduction, phase transition or solid solution formation. In this way reaction caused by impurities, additives or other product formed during heating which are often included in the normal sintering process may imply some sort of reactive sintering which usually generates additional porosity. This sintering process is complicated because the phase changes are involved. Thus the understanding of material behaviors such as binder burnout, densification mechanisms of LTCC, pore evolution and deformation of suspended LTCC is important in optimizing the fabrication process for multilayer LTCC substrates as well as for tailoring new LTCC systems (Kemethmuller et al., 2007).

Sample	Density (g/cm^3)	Porosity (%)	Shrinkage (X)/%	Shrinkage (Y)/%	Shrinkage (Z)/%
800	2.992	0.92	14.13	13.28	23.13
825	2.873	4.97	14.35	13.67	22.74
850	2.910	3.64	14.41	14.00	21.56
875	2.860	5.29	15.06	15.15	21.16
900	2.806	7.08	14.53	13.99	21.85

Table 2. Physical properties of LTCC tape samples fired at various sintering temperature.

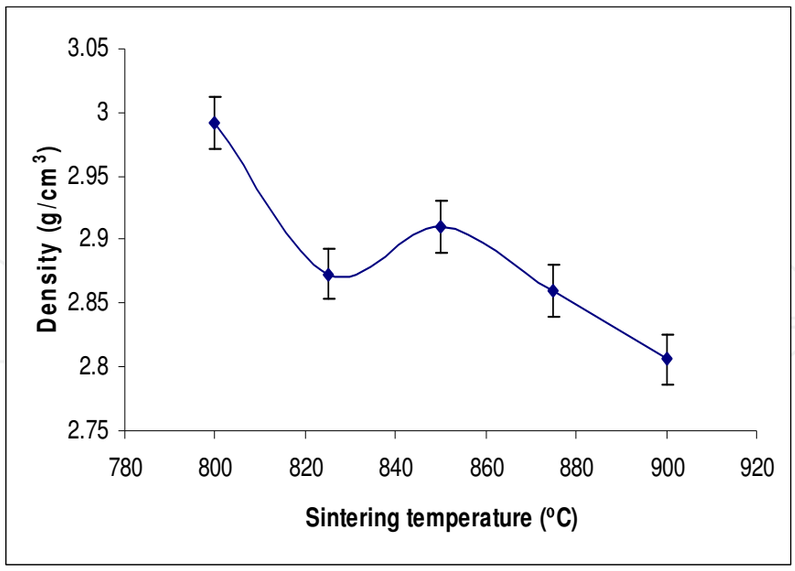

Fig. 4. The plot of the density with the variation of sintering temperature for substrate with metal conductor.

According to the Ferro guideline the tape A6S used in this work is a crystallizing Ca-B-Si-O system and CN33-391 used as a thick-film material (Ferro; Muralidhar et al., 1992). Both of them typically consist of glass and/or oxide dispersed in organic medium. Owing to the coexistence of ceramic filler and glass in LTCCs, liquid phase sintering can be considered; due to the large amount of glass, viscous sintering can be assumed, so the liquefaction of glass has a dominant role. The presence of these mechanisms increased the volume and size of pores inside the material. The density drop due to porosity is based on the same weight for all the samples i.e.; for $\rho = \frac{M}{V}$; M does not change but V increases to accommodate higher porosity (more pores) within the samples. However in the present case, the porosity present inside the substrate cannot support the decreasing trend of density with increasing sintering temperature. So, it is believed that the main reason of the decreasing trend of the density with increasing sintering temperature could be due to the chemical reaction e.g. between some components such as silver in the system with the oxygen. The chemical reaction can result in an expanded volume for the system. Referring back to the XRD analysis in Fig. 3, increasing sintering temperature the phases of Calcium Silicate ($CaSiO_3$) become more stable with the highest intensity for each samples. This phase has the lowest theoretical density (2.92 g/cm^3) among other phases. This finding was consistent with the results found by Erol and his co-workers in 2009 from their studies on the influence of the binder on the properties of sintered glass-ceramics produced from industrial wastes (Erol et al., 2009). They concluded that the densities of the sintered glass-ceramic samples changed depending on the amount of crystalline phase. The higher the content of crystalline phases with high density, the higher the measured density; the higher the amount of crystalline phase with the lower density, the lower the measured density will be obtained. So this might be a reason why the decreasing density was obtained in this present work.

3.2.2 Linear shrinkage

In general, dimensional control is a fundamental problem in ceramic processing. In this co-fired package the dimensional control, reproducibility and consistency of the shrinkage value to exact tolerance are strongly required and critical. Better reproducibility increases the uniformity of finished product characteristics and thereby increases the process yield. Each process step must complement the preceding and subsequent steps to achieve reproducibility. The main factor governing the reproducibility is the control of shrinkage. This rigid dimensional control in terms of shrinkage is the key to manufacturing high quality, high yield LTCC devices especially when the dimensions of lines and vias continuously decrease. Furthermore, repeatable shrinkage results are also needed for accurate positioning of circuit features such as vias, landing pads, cavities, surface mount component placement and post-fired printing and testing alignment (Sawhill, 1988). Dimensional uncertainties can result in disregistries of the laminated substrate due to the difficult control of the shrinkage amount (Raj and Cannon, 1999). So, to achieve desired properties and desired dimension, the process engineer must establish control of critical process variables.

It is clear that the linear shrinkage as tabulated in Table 2 increases up to 875 °C and drops slightly at 900 °C. It was due to the reactivity of the cofired material components such as ceramic oxide, glass, metal and organic solvent. This reaction also depends on the firing condition such as temperature, time and ambient atmosphere (Rabe et al., 2005). Typically, the shrinkage of the LTCC substrate across its width (XY) will be nearly identical while for the Z direction it has big variations. In the commercial practice, the standard values for XY and Z shrinkage are about 14-17 % and 20-25 % respectively. In this work the shrinkage was about 13-15 % for XY and 21-24 % for Z direction (Table 2). Chiang et al. (2011) has noted that in his work the shrinkage in the thickness direction is always larger than that in-plan shrinkage due to more organic material accumulated on the top surface of the green tape caused by unidirectional drying. However for the XY direction the better particle packing is believed to reduce shrinkage during sintering.

3.3 Microstructure

Microstructural characterization of ceramic packaging materials plays an important role in the understanding and improvement of most material properties such as thermal, electrical and mechanical properties (Pinckney and Beall, 2008). The properties of LTCC material are determined not only by the chemical composition and crystal structure but are also governed by the microstructural features such as density, grain size, porosity, intra- and inter-granular pore distribution, phases, crystalline morphology, crystallography and the chemistry of the interfaces. Such a microstructural arrangement can produce property inhomogeneities. The inhomogeneities usually occur during sample preparation. Brook (1988) has start earlier investigation on the role of inhomogeneities in the sintering process of alumina. Since early work on the subject, abnormal grain growth in alumina has often been attributed to inhomogeneities. He also noted that there are two principal kinds of inhomogeneities that may exist in a green or sintered body; extrinsic and intrinsic. Extrinsic inhomogeneities are associated with imperfect processing such as chemical segregation during drying, agglomeration or defect in powder consolidation. Intrinsic inhomegeneities are associated with anisotropy in the material. In a later investigation by Cho et al., (2000)

and Sone et al., (2001) has shown that the impurity inhomogeneities in alumina would also produce abnormal grain growth. So, the desirable properties at particular frequencies can be improved by carefully controlling of the microstructure where the change of microstructure is the main issue in engineering materials.

3.3.1 Grain growth

One of the microstructural aspects normally studied is the grain growth. To date there exists a fairly detailed understanding of how grains of a sintered material can grow. According to Kingery (1976) the normal grain growth is the process by which the average grain size of the material increases continuously without a change the graphical shape of the grain size distribution during the heat treatment. Grain growth in polycrystalline materials is conventionally considered to be the results of the migration of grain boundary in response to the driving force provided by the system energy associated with the reduction in the total interface area by interface migration (Dillon and Rohrer, 2009). Since mass is conserved, some grains get smaller and disappear while others grow larger. In grain growth, the fundamental process is transferring an atom across the boundary from one grain to another as shown in Fig. 5. In this respect, it is well known that sintering is an interfaced related process in terms of driving force (Jo et al., 2006). This curvature–drive motion of grain boundary can lead to a normal behavior.

The occurrence of grain growth involves the elimination of free surface, i.e. the elimination of pores during sintering and is one of the ways in which there occurs a spontaneous decrease in the free energy during heating of a system with large interfacial areas (Pampuch, 1976). Interface energy is associated with the boundary between individual grains. A decrease in the free energy of such a system is also possible when the area of interfaces between the grains (grain boundary) decreases because of the excess energy possessed by these boundaries. The decrease in the area of the grain boundaries means an increase in the size of the grains. This is possible when some grains grow at the expense of others as the consequence of the movement of the grain boundaries toward their centers of their curvature. The boundary velocity has been observed to be linearly dependent on the curvature. This phenomenon can be explained in terms of the capillary force. The driving force for the grain growth process is the difference between the fine grain material and the larger grain size product resulting from the decrease in grain boundary area and the total boundary energy (Kingery, 1976). Grain growth must be controlled by even significant defects of the texture of the poly-crystal. It may be stopped by the presence of foreign inclusions (Shackelford, 1992). Besides the solid phase inclusions, the most important influence is exerted by pores (inclusion of gaseous phase). This explains the fact that, in some cases, grain growth does not take place at all, or wherever it is observed, it takes place only after the elimination of most of the pores, or after a considerable decrease in the volume fraction of pores on sintering.

Atoms can move across the grain boundary as well as within crystals when heated at high temperature. Equal numbers of atoms cross a plane boundary in opposite directions. However, atoms on a concave-surfaced boundary are likely to have more neighbors, and hence less energy than atoms on a convex-surfaced boundary. This brings about the chemical potential of the atoms. This causes a movement of the boundary towards the center

of its curvature (See Fig. 5). Owing to this movement the grain growth takes place i.e. an increase in the size of the grains with many neighbors at the expense of grains with few neighbors.

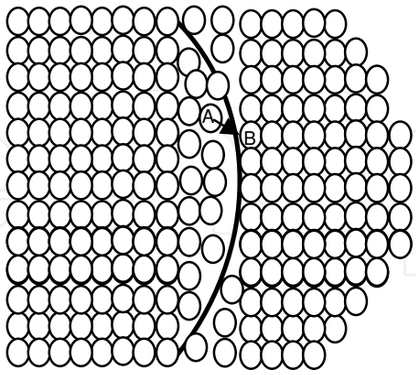

Fig. 5. Classical picture of a grain boundary.

Across the curved grain boundaries, there is the difference in the chemical potential resulting from the stresses which should be directed from the concave side of the curved interface to its convex side. Thus atoms on the convex side are in a state of compression and those on the concave side are in tension. This brings about a change in the chemical potential of the atoms (Rahaman, 1995). The gradient of the chemical potential constitute the driving force for the process of transferring atoms from the convex to the concave side across the curved grain boundary; this causes the movement of the boundary towards the centre of its curvature i.e. in a manner increasing the radius of the curvature. Owing to this movement, grain growth takes place, i.e. an increase in the size of the grains with many neighbors at the expense of grains with few neighbors. The rate of growth is proportional to the driving force and the driving force is proportional to the total amount of grain boundary energy. The driving force for each crystal to grow or shrink is given by the free energy difference between the atoms on the convex side and its difference across the interface amounts which given by the equation 7,

$$\Delta G = \gamma \overline{V} \left(\frac{1}{r_1} + \frac{1}{r_2} \right) \tag{7}$$

Where ΔG is the change in the free energy on going across the curved interface, γ is the boundary energy $\overline{V}$ is the molar volume and r_1 and r_2 are the principal radii of the curvature.

3.3.2 Glass-ceramic tape microstructure

Glass-ceramics formed by the controlled nucleation and crystallization of a glass precursor. As mention in the previous section, the Ferro A6S tape system consists of ceramic filler in glass matrix. The formation of a liquid phase is helpful to improve the development of microstructure behavior of the substrate. For glass-ceramics based on internal nucleation and grain growth, a general evolutionary pattern is observed in the crystallization cycle: amorphous phase separation and/or precipitation of primary crystalline nuclei, nucleation

and growth of metastable crystalline phases and approach to a stable crystalline structure (Pinckney and Beall, 2008). Amorphous phase separation is generally the first stage in glass-ceramic formation. This phase is highly unstable as a glass and will precipitate primary crystalline nuclei on heating at temperature near the annealing point of the host glass. The next nucleation stage usually involves the heterogeneous nucleation and growth of metastable crystalline phases on the primary crystalline nuclei, resulting in a fine-grained metastable solid solution assemblage. Finally with increasing temperature, this metastable phase assemblage breaks down into stable crystalline phases by means of crystal phase transformation, reaction between metastable phases or a combination of several of these mechanisms.

The effects of sintering temperature on microstructure of glass-ceramic tape are shown in Fig. 6. It is clearly seen that there is inhomogeneous microstructure for the entire sample with some sample showing a big size pore meaning that probably only a few crystallite sizes present in the bulk samples. This feature of the microstructure could be due to the agglomeration within the sample. In the LTCC process, some particles are densely packed and some particles are loosely packed due to the agglomeration of particle at some places. The presence of agglomeration is a common problem in ceramics processing and influenced the microstructure behavior of the whole substrate. As mentioned by Lange (1984) and Hirata et al., (2009), when a laminated substrate or powder compact is heated, the inhomegeneity of the packing provides the different densification rate and the produce a microstructure which is usually not uniform when agglomeration is severe. An inhomogeneous distribution of particles leads to an inhomogeneous liquid distribution such that there is no driving force for redistribution of the liquid, so the densification rate is not homogeneous and the microstructure development also becomes inhomogeneous.

Based on their research, Deng et al., (2007) studied the microstructure of porous ZrO_2 ceramics and found that the agglomeration resulted in localized non-uniform shrinkage and the large pores are believed to originate from the large interagglomerated particles and greater microstructure non-uniformity. The agglomerated tape however leads to lower densities with large shrinkage deviations in particular direction giving a poor quality (Raj and Cannon, 1999). Agglomeration promotes uneven sintering which sometimes results in a mechanically weak and porous product. Thus, to achieve a high density material and good microstructure development, the agglomeration needs to be controlled (Forrester et al., 2008).

The densification process of the glass-ceramic composite can be described by the conventional three-stage liquid phase sintering; particle rearrangement, dissolution and precipitation and solid state sintering. The presence of glass in this composite system, acts as a sintering aid which produces liquid phase formation at a temperature lower than the sintering temperature and may considerably increase the rate of sintering. The viscous liquid which occurs during the sintering process may promote an additional diffusion mechanism of dissolution/precipitation, particle rearrangement and capillary forces and finally affect the densification at high temperature. Compared to the solid state sintering, liquid phase sintering enhances densification by two mechanisms; the densification is caused by mass transport via lattice diffusion from grain boundaries and grain boundary diffusion that should be encouraged to obtain high density when the sintering temperature is increased.

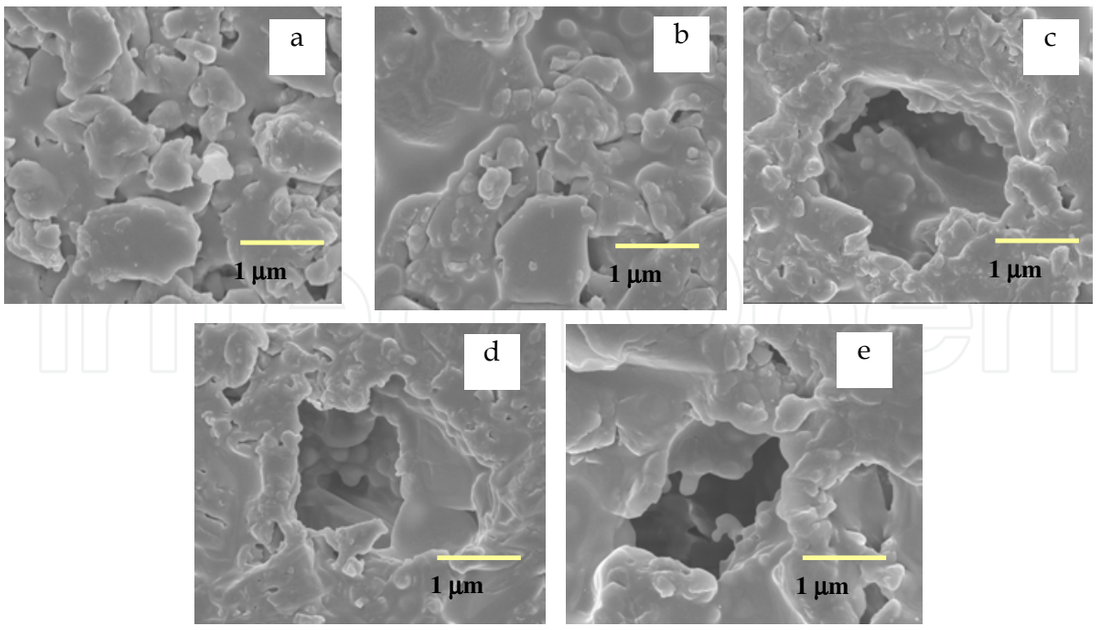

Fig. 6. SEM micrograph of laminated sample sintered at a) 800 °C, b) 825 °C, c) 850 °C, d) 875 °C and e) 900 °C.

The whole densification rate at the final stage, is a summation of the developed local internal defect such as the presence of pores that are no longer large enough to prevent grain growth and this is the major process going on in addition to the final densification. With the increasing grain size, the densification rate decreases as the distance of the defects to the grain boundaries increases. Grain growth also gives pore coalescence where smaller pores are merged together into larger ones: this also reduces the densification rate and explains the density results obtained. In the case of the sintering process of glass ceramic material, if crystallization occurs before densification, the viscosity of samples will be increased. It is due to the contribution of glass composition into a crystalline phase structure, resulting in the reduction of viscous flow of the system. As a result, densification through viscous flow sintering will not occur properly and a porous body will be formed (Banijamali et al., 2009).

3.3.3 Silver grain microstructure

In the LTCC technology, the microstructure changes involves the combination of a substrate and conductor material where LTCC tape materials contain a glass binder and organic solvent for tape casting purpose, thick-film conductor also contain glass frit as adhesion element with the substrate via formation of a vitreous bond (Kuromitsu et al., 1994). However, knowledge about the interaction of ceramic filler and amorphous matrix is very limited. Moreover the understandings of how an amorphous matrix influence the crystal grain growth in the metal film is not yet clear (Liu and Shen, 2004). According to Yajima and Yamaguchi (1984) the densification process of the substrate and printed film are depends upon sintering where the conductor and the substrate consisting of CaO-B_2O_3-SiO_2 sinter simultaneously. So the liquid phase formed is believed to help densification of metal powder to a denser packing of grains (see Fig. 7).

The SEM micrograph observation of microstructural changes of silver with sintering temperature is shown in Fig. 7. As observed here, the distribution of silver grain size is not homogenous; some grains have grown pretty well and some grains have not. There are relatively small grains about 2-4 μm in size coexisting with many large grains about 8-12 μm. It was also noted that the grain morphology are non-uniform/irregular shape. There are many curved boundaries and there is little obvious faceting or shape anisotropy in certain areas. Verhoeven (1975), has stated that generally two factors influence the shape of grains; the requirement to fulfill space and to be in a state of metastable equilibrium particularly with regard to the total grain boundary surface area. So the net result is that the three dimensional grains are irregular polyhedron with curved faces. Kang et al., (1985) has revealed that the grain shape changed mainly due to the anisotropic grain growth of grains rather than by contact flattening as suggested by Kingery's model. The distribution of the glass-frit diffusion is an inhomogeneous manner; the distribution of the metal grain will be varied. The quality of silver thick-film is dependent on the properties of the bottom substrate. Rane et al., (2003) reported that the microstructure changes in thick film that occurs during firing depends primarily on the sintering of silver powders as well as on the glass bonded interaction presuming that the substrate material has a slight influence on the sintering and microstructure. In LTCC materials, the LTCC substrate also plays an important role in the development of the microstructure during sintering since it is a co-firing process where the conductor and the substrate were fired together. Moreover the microstructural changes in the conductor film during the co-firing process also depend strongly on the sintering of metal powders, binder material interaction and the decomposition of the binder present in both paste and LTCC tape materials which lead the formation of cavities /voids on the surface of the fired film (Bangali et al., 2008).

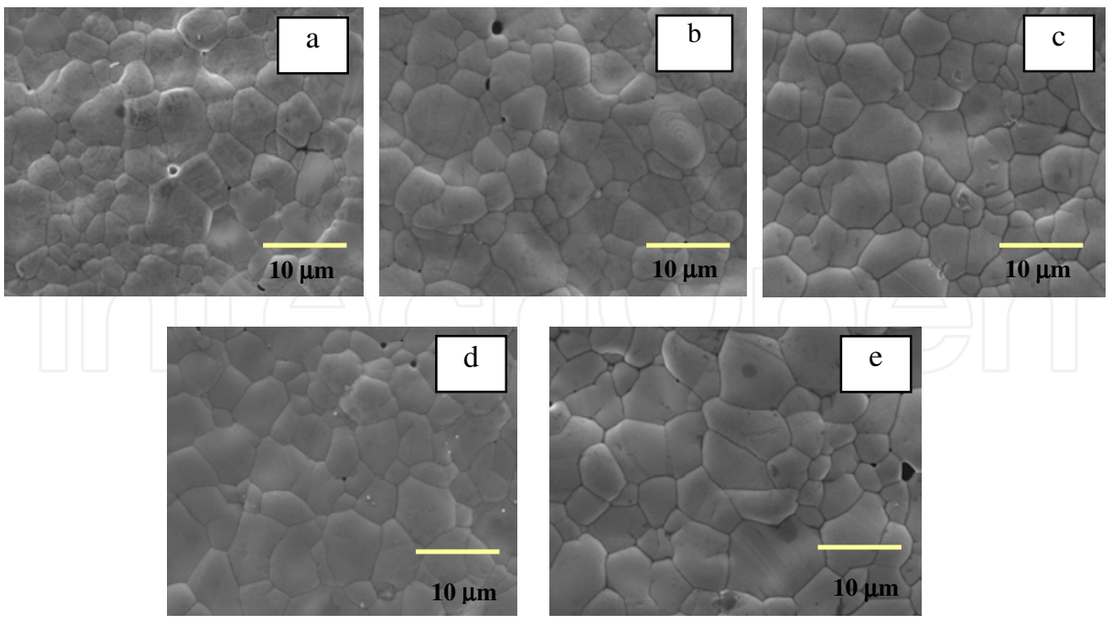

Fig. 7. SEM micrograph of silver surface sintered at a) 800 °C, b) 825 °C, c) 850 °C, d) 875 °C and e) 900 °C.

The tape system as a support substrate for printed metal contain SiO_2 and Ca or a combination of $CaSiO_3$ as observed in XRD peak in the samples would cause some defects in microstructure due to the formation of liquid phase. As reported by Louet et al. (2005), the SiO_2 content can increase the sintering rate due to the formation of an intragranular vitreous phase while the combination of CaO and SiO_2 is responsible for abnormal grain growth. As the contents of SiO_2 and Ca or a combination of $CaSiO_3$ increase at some places, they should increase the grain growth kinetics due to the formation of liquid phase which preferentially fill the spaces between the solid particles. It is indicated that the liquid phase has excellent wettability with $CaSiO_3$. Therefore the silver powder was sintered with liquid glass phase. When the $CaSiO_3$ becomes liquid, chemical reactions such as the migration of silver into the liquid frit would occur on the surface of silver. It also believes that the silver conductive thick-film contains about 90 wt% silver and 10wt % glass frit. So, the presence of the liquid phase gives rise to changes of its atomic mobility and is known to be the cause of abnormal grain growth. During sintering process, the glass phase may decompose into liquid phase providing the capillary force for neighboring particles to come closer and react. If the glass phase is not uniformly distributed, the grain growth is not homogeneous.

The average grain size of sintered body was measured over 200 grains by the linear intercept method. Fig. 8 was plotted with varied sintering temperature for the average grain size and the density of the substrate. As we can see with increase the firing temperature, the silver grains grow in much good shape up to 900 °C and the average grain size increased from ~4.39µm to ~5.60 µm. The work is consistent with the findings by Huang and Tsai (2001), which noted that the grain size increases with increasing sintering temperature.

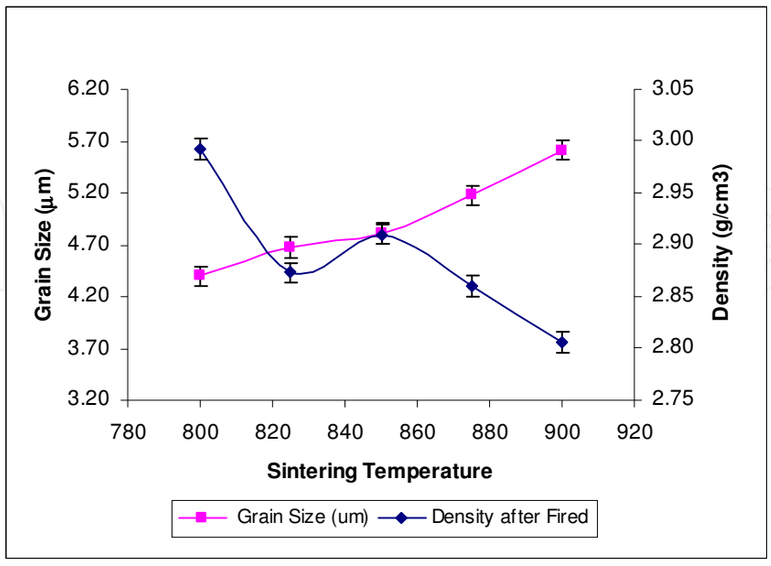

Fig. 8. Average grain size of printed conductor fired at various sintering temperature.

However, the trend of the average grain size (metal surface) and the density (whole substrate) are somewhat opposing trend with increasing sintering temperature. The relation of microstructural changes with decreasing density is not significant in this work because the density is highly extremely extrinsic and macroscopic property while the average grain size is less extrinsic and microscopic average of crystallite size in polycrystalline material.

The average grain size can be increased when increasing the sintering temperature however the density does not always show a similar trend of the average grain size with increase the temperature due to the presence of pores and other defects or stresses within the sample (Alias et al., 2009). The average grain size of a sintered product is influenced by the total shrinkage characteristic during sintering. The glass contained in metal thick-film formed the liquid phase during sintering resulting in faster grain growth speed of the conductor because of its excellent low temperature shrinkage characteristics. The increase of average grain size shows the microstructural evolution of the samples. These can be either be intrinsic effects related to the crystal structure, defect, surface or energy anisotropy of the material or be extrinsic such as pore size, density heterogeneity, partial wetting by the liquid phase and preferential impurity (Feteira and Sinclair, 2008) . The microstructure of printed silver metal can be designed to attain the features such as fine grain size, low porosity and negligible second phase that can improve operation at the particular frequency. The control of microstructure of metal films is very important for a good device performance.

The microstructural evolution of the sintered samples can be described by adapting the sintering mechanism explained by Sameshima et al. (2000). There are 5 stages involved in the process:

1. First initial stage where no grain growth and mass transport of the sintered samples occur by grain boundary diffusion.
2. Second initial stage occurs afterwards where no grain growth occurs and the mass transport of sintered body is by lattice diffusion.
3. First intermediate and final stage later takes place where lattice diffusion occurs without any grain growth of the samples.
4. Second intermediate and final stage where there is grain growth happening and lattice diffusion still playing its role.
5. Final intermediate stage where grain boundary diffusion occur with no grain growth.

Microstructure evolution has a large influence on the material properties generally and can be characterized by abnormal grain growth behavior where a few selected grains grow by replacing the other grains (Ubach et al., 2004). The main cause of the abnormal growth is due to the presence of anisotropy of either the surface energy or the strain density (Paik et al., 2003). Anisotropy of the grain boundary energy has been considered to be origin of the abnormal grain growth observed in bulk materials. It is possible that this may apply to the silver film. The silver grain growth mechanism could be evaluated according to its activation energy (Q). Coble's theory in Coble (1961) mentioned that from the behavior of particle growth, the activation energy of metal grain growth can be predicted using Arrhenius equation as below:

$$d\ln k/dT = Q/RT^2 \tag{8}$$

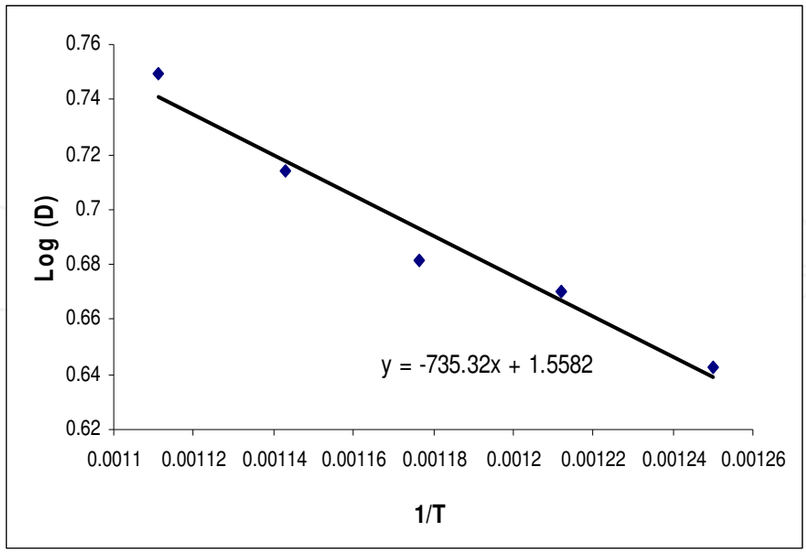

Fig. 9. Plots of log D versus the reciprocal of absolute temperature (1/T).

where k is the specific reaction rate constant, Q is the activation energy, T is the absolute temperature, and R is the ideal gas constant. The value of k however can directly be related to grain size according to Jarcho et al. (1976), which resulted in the equation below:

$$LogD = (-Q / 2.303R)1/T + A \tag{9}$$

Where T is the absolute temperature, A is the intercept and D is the grain size. By using equation 9, one can obtain a best fitted straight-line plot of grain size where a plot of log D versus the $1/T$ as shown in Fig. 9. From the equation (9), we obtained the slope of the line which is $-Q/2.303R$ and the value of the activation energy of metal grain growth (Q) can be calculated from the Arrhenius plot which is 14.079kJ/mol which might be ascribed to grain boundary grooving, precipitation, impurity drag or interfacial reaction between the films and the substrate. The obtained values is considered too low compared to the activation energy calculated by Wu et al. (2011) from their studies on the behavior of ZnO-doped silver thick-film and the silver grain growth mechanism.

3.3.4 Anisotropic grain growth

A closer look for sample sintered at 800 °C and 825 °C as shown in Fig. 10, we clearly see pronounced layered-structure grain growth/faceted grain microstructure. The large relatively faceted grains have differed orientations between each other. For the oriented grain growth the preferred direction is the same for all directions. So in this case, the anisotropic structure occurs for a restricted number of grains and can be due to the crystallographic effects. For all cases of the direction growth of anisotropic grain is random. Growth anisotropy is produced naturally during the process of grain growth (Uematsu et al., 1997).

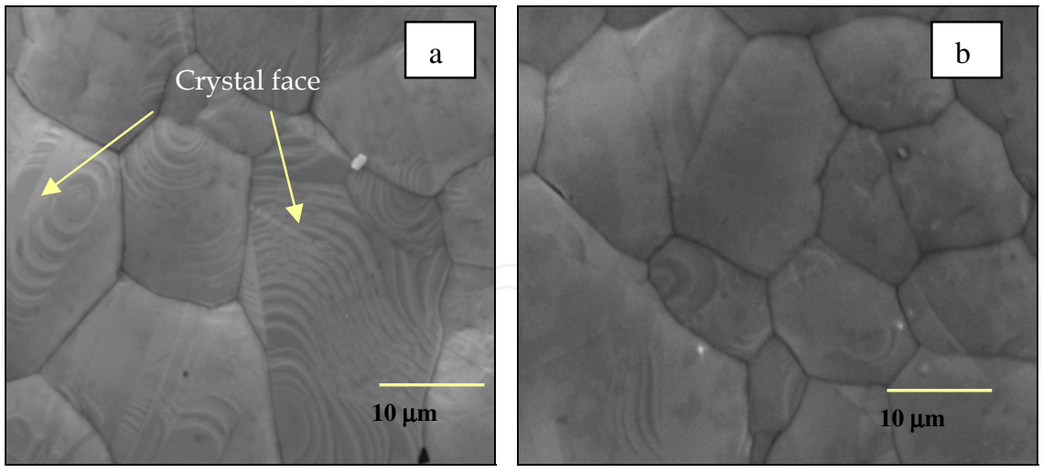

Fig. 10. Anisotropic grain microstructure for sample sintered at a) 800 °C and b) 825 °C.

There are some investigations on the anisotropic grain growth as well as the presence of faceting grain of alumina interface in the presence of glass (Simpson and Carter, 1990). The faceting of alumina interface in the presence of a glass is a factor affecting the grain boundary movement during sintering. The geometry and movements of facet during liquid phase sintering process are expected to influence directly the final microstructure of the grain boundaries that ultimately control the properties of the alumina compact.

For a faceted grain in a liquid matrix, the dihedral angle is not uniquely defined because of the torque on a facet, contrary to the case of a rounded grain. When two faceted grains are in contact with a certain angle of crystallographic orientation in a liquid matrix, the shape of the contact boundary in equilibrium must be that of the minimum interfacial energy. These abnormal grains originate from heterogeneities in the chemical composition, particle size and packing density. In the LTCC process, the substrate also plays an important role in the development of microstructure during sintering since it is a co-firing process where the conductor and the substrate are sintered simultaneously. So, the nuclei of abnormal grains may be formed during different stages of sintering. From XRD peak observation for samples sintered at 800 °C and 825 °C, a few phases including $CaSiO_3$ and $Ca_3(SiO_4)O$ were present suggesting the nucleation rate is not zero. The results found was consistent with the work of Rohrer (2001) which noted that at lower temperature, the anisotropy grain of the surface energy is expected to be higher. The wollastonite phase ($CaSiO_3$) becomes a liquid phase before it decomposes. The liquid phase exists preferentially, filling spaces in small pores and particle contact. The capillary force that is generated by the liquid phase can drag the nearby particle close together. The distribution of the liquid phase may not be uniform because the amount of liquid is small. According to Kang et al, (1991), liquid phase, even in a small amount forms due to the presence of impurities, grains are faceted and abnormal grain growth occurs. Such heterogeneities may trigger the formation of nuclei of abnormal grain. Because the nuclei are small, they have a greater chance to grow at their own pace until they encounter other abnormal grains (Chen and Tuan, 2000). However, when a liquid phase forms due to a high concentration of impurities, the grain shape is faceted and abnormal grain growth

occurs at low annealing temperatures. The edges of faceted grains become rounded with an increase in annealing temperature and normal grain growth occurs because of an increased contribution of entropy (a reduction of self free energy). Critical amounts of CaO and SiO_2 to induce and to suppress abnormal grain growth were also measured. According to the results, when the amounts of CaO and SiO_2 are within their solubility limits, normal grain growth occurs. On the other hand, abnormal grain growth occurs if the amount is above the solubility limit.

With increasing temperature, the faceted grain microstructure becomes less prominent. It might be due to the presence of boundary defect. As studied by Maclaren et al. (2003), all faceted microstructure being limited by a paucity of steps, ledges or boundary dislocation to serve as site for atom attachment or detachment. As the sintering temperature increases the faceted or anisotropic microstructure are limited. Although the faceted grain microstructure observed is not large, the effects on surface morphology are significant. Furthermore it should be pointed out that there is geometry limits to observable anisotropies for perpendicular surface in any equilibrium experiment.

4. Conclusion

As a conclusion, the performance of the laminated sample strongly depends on the starting raw materials and processing method; good technical skills and handling procedures are required to minimize the defect/issue occurring in the LTCC multilayer process. As with other advanced electronic ceramics, the quality of raw materials will have a marked effect on the final properties of a ceramic product. The raw material selection includes characterization of purity, particle size distribution, surface area, consistency and cost. The processing of a ceramic material must be optimized with respect to microstructural characteristics, because only by this way we can produce ceramics with properties that approach the level of intrinsic dielectric properties. The chosen raw material is the first key to controlling the microstructure and making a consistent product.

The present study is able to explain the effect of the different sintering temperatures on the whole substrate properties and printed thick-film. The microstructural evolution at various sintering temperatures was carefully tracked. The sintering temperature therefore plays a vital role in forming microstructures, porosity and shrinkages of the as-prepared materials. This is more complex than the simple sintering of metal grains. In order to understanding better the microstructure evolution, the study of samples fired should be carried out at the different stages of the sintering process. This work will be very helpful to predict how the microstructural factors and material properties of the LTCC system would affect the microwave-frequency performance of relevant devices. It should be mentioned that the results obtained from this work is not always be consistent with observations from other works.

5. Acknowledgement

The authors wish to thank Telekom Malaysia for their funding support under project IMPACT (RDTC/100745) and Assoc. Prof. Dr. Mansor Hashim, Mr. Ismayadi Ismail and Mrs. Sabrina Mohd. Shapee for the guidance and support for this research work.

6. References

Alias, R., Ibrahim, A., Shapee, S.M., Ambak, Z., Yusoff, Z.M. and Saad, M.R. (2009). Microstructure and Thermal Diffusivity of Al_2O_3-SiO_2-Based Substrate with Varied Sintering Temperatures. *Journal of the Australian Ceramic Society,* Vol. 45, No. 2, pp. 80-84.

Bangali, J., Rane, S., Phatak, G. & Gangal, S. (2008). Silver Thick-Film Paste for Low Temperature Co-fired Ceramic: Impact of Glass Frit Variation. *Soldering and Surface Mount Technology*, Vol. 20, No. 3, pp. 41-46.

Banijamali, S., Eftekkhari Yekta, B., Rezaie, H.R. & Marghussian, V.K. (2009). Crystallization and Sintering Characteristics of CaO-Al_2O_3-SiO_2 Glasses in the Presence of TiO_2, CaF_2 and ZrO_2. *Thermochimica Acta*, Vol. 488, No. 1-2, pp. 60-65.

Barlow, F.D. & Elshabini, A. (2007). *Ceramic Interconnect Technology Handbook*. CRC Press, New York.

Brook., R. J., Tuan, W.H and Xue, L. A (1988) Critical Issues and future directions in sintering science Ceramic Transaction 1, pp; 811-823.

Chang, C.-R. & Jean, J.-H. (1998). Effect of Silver Paste Formulation in Camber Development during the Co-Firing of Silver Based LTCC Package. *J. Am. Ceram. Soc.*, Vol. 81, No. 11, pp. 2805-2814.

Chang, C.-R. & Jean, J.-H. (1999). Crystallization Kinetics and Mechanism of Low-Dielectric, Low Temperature, Cofirable CaO-B_2O_3-SiO_2 Glass Ceramics. *J. Am. Ceram. Soc.*, Vol. 82, No. 7, pp. 1725-1732.

Chen, C-.S., Chiou, C.-C., Chen, C.-S. & Lin, I.-N. (2004). Microwave Dielectric Properties of Glass-MCT Low Temperature Cofireable Ceramics. *J. European Ceramic*, Vol. 24, pp. 1795-1798.

Chen, C.-Y. & Tuan, W.-H. (2000). Effect of Silver on the Sintering and Grain Growth Behavior of Barium Titanate. *J. Am. Ceram. Soc.*, Vol. 83, No. 12, pp. 2998-2992.

Chiang, M.–J., Jean, J.-H. & Lin, S.-C. (2011). The Effect of Anisotropy Shrinkage in Tape-Cast Low Temperature Co-Fired Ceramics on Camber Development of Bilayers Laminates. *J. Am. Ceram. Soc.*, Vol. 94, No. 3, pp. 683-686.

Cho, S.-J., Kim, K.H., Kim, D.J and Yoon, K.J. (2000). Abnormal Grain Growth at the Interface Centrifugally Cast Alumina Bilayer during Sintering, *J. Am. Ceram. Soc.*, No. 83, pp. 1773-1776.

Coble, R.L. (1961). Sintering Crystalline Solids. I. Intermediate and Final State Diffusion. *J. Appl. Phys.*, Vol. 32, No. 5, pp. 787-792.

Deng, Z.-Y., Fereira, J.M., Tanaka, Y. & Isoda, Y. (2007). Microstructure and Thermal Conductivity of Porous ZrO_2 Ceramics. *Acta Materialia*, Vol. 55, pp. 3663-3669.

Despande, V., Kshirsagar, A., Rane, S., Seth, T., Phatak, G.J., Mulik, U.P. and Amalnerkar, D.P. (2005). Properties of Lead-Free Conductor Thick-Films of a Co-Precipitated Silver Palladium Powders. *Materials Chemistry and Physics,* No. 93, pp. 320-324.

Dillon, S.J. & Rohrer, G.S. (2009). Mechanism for the Development of Anisotropy Grain Boundary Character Distribution during Normal Grain Growth. *Acta Materialia*, Vol. 57, pp. 1-7.

Erol, M., Kucukbayrak, S and Ersoy-Mericboyu, A. (2009). The Influence of the Binder on the Properties of Sintered Glass-Ceramics Produced from Industrial Wastes. *Ceramics International*, No. 35, pp. 2609-2617.

Ferro Corporation; Ferro Design Guideline in www.ferro.com.

Feteira, A. & Sinclair D.C. (2008). Microwave Dielectric Properties of Low Firing Temperature $Bi_2W_2O_9$. *J. American Ceram. Soc.*, Vol. 91, No. 4, pp. 1338-1341.

Forrester, J.S., Goodshaw, H.J., Kisi, E.H., Suaning, G.J. & Zobec, J.S. (2008). Effect of Milling on the Sintering Behavior of Alumina. *J. Am. Ceram. Soc.*, Vol. 44, No. 1, pp. 47-52.

Hirata, Y., Hara, A. & Aksay, A. (2009). Thermodynamics of Densification of Powder Compact. *Ceramics International*, Vol. 35, pp. 2667-2674.

Hrovat, M., Balavic, D, Kita, J., Holc, J, Cilensek, J. and Drnovsek, S. (2009). Thick-Film Thermistors and LTCC Materials; The Dependence of the Electrical and Microstructural Characteristics on the Firing Temperature. *J. of Europ. Ceram. Soc.*, 29, pp. 3265-3271.

Hsi, C.-S, Chen, Y.-R and Hsiang, H.-I (2011), Diffusivity of Silver Ions in the Low Temperature Co-fired Ceramic (LTCC) Substrate. *J. Mater. Sci*, Vol. 46, Issue 13, pp. 4695-4700.

Hsu, Y.-F, Wang, S.-F & Cheng, T.-W. (2003). Effects of Additives on the Densification and Microstructural Evolution of Fine θ-Al_2O_3 Powder. *Mat. Sc. & Eng. A*, Vol. 362, Issue 1-2, pp. 300-308.

Hsueh, C. H. and A. G. Evans. (1985). Residual Stress and Cracking in Metal/Ceramic Systems for Microelectronics Packaging, *J. Am. Ceram. Soc.*, No. 68, Vol. 3, pp. 120–127

Huang, C.-L. & Tsai, J.-T. (2001). Effects of Sintering Temperature on CaO-Li_2O-Sm_2O_3-TiO_2 Microwave Dielectric Ceramic. *Proc. Natl. Sci. Counc. ROC (A)*, Vol. 25, No. 5, pp. 317-321.

Imanaka, Y. & Kamehara, N. (1992). Influence of Shrinkage Mismatch between Copper and Ceramics on Dimensional Control of the Multilayer Ceramic Circuit Board. *J. Ceram. Soc. Jpn. Int. Ed.*, Vol. 100, pp. 558-561.

Imanaka, Y. (2005). *Multilayered Low Temperature Co-fired Ceramic (LTCC) Technology*. Springer, New York.

Jarcho M., Bolen C.H., Thomas M.B., Bobick J., Kay J.F., Doremus R.H. (1976) Hydroxylapatite Synthesis and Characterization in Dense Polycrystalline Form. *Journal of Materials Science*. Vol.11, No. 11, pp. 2027-2035.

Jean, J.-H and Fang, Y-C., Dai S. X. and. Wilcox, D. L. Sr. (2001) Devitrification Kinetics and Mechanism of K_2O–CaO–SrO–BaO–B_2O_3–SiO_2 Glass-Ceramic. *J. Am. Ceram. Soc.*, Vol. 84, No. 6, pp. 1354–1360.

Jean, J.-H., Chang, C.-R. & Lei, C.-D. (2004). Sintering of Crystallizable CaO-B_2O_3-SiO_2 Glass with Silver. *J. American Ceram. Soc.*, Vol. 87, No. 7, pp. 2630-2633.

Jo, W., Kim, D.-Y. & Hwang, N.-M. (2006). Effect of Interface Structure on the Microstructural Evolution of Ceramics. *J. Am. Ceram. Soc.*, Vol. 89, No. 8, pp. 2369-2380.

Kang, S.-J.L., Kaysser, W.A., Petzow, G. & Yoon, D.N. (1985). Growth of MO Grains around Al_2O_3 Particles during Liquid Phase Sintering. *Acta Metall.*, Vol. 33, pp. 1919-1926.

Kang, S.-J.L., Kim, K.-H. & Yoon, D.N. (1991). Densification and Shrinkage during Liquid Phase Sintering. *J. Am. Ceram. Soc.*, Vol. 74, No. 2, pp. 425-427.

Kemethmuller, S., Hagymasi, M., Stiegelschmitt, A. & Roosen, A. (2007). Viscous Flow as the Driving Force for the Densification of Low Temperature Co-Fired Ceramic. *J. Am. Ceram. Soc.,* Vol. 90, No. 1, pp. 64-70.

Kingery, W.D., Bowen, H. K., & Uhlman, D.R. (1976). *Introduction to Ceramics*, (2nd Ed.), John Wiley and Sons, New York.

Klug, H.P. & Alexander, L.E. (1974). *X-Ray Diffraction Procedures for Polycrystalline and Amorphous Materials*. John Wiley and Sons, New York.

Kume, S., Yasuoka, M., Lee, S.-K., Kan, A., Ogawa, H. And Watari, K. (2007). Dielectric and Thermal Properties of AIN Ceramics. *J. Europ. Ceram. Soc.*, Vol. 27, pp. 2967-2971.

Kuromitsu, Y., Wang, S.F., Yoshikawa, S. & Newnham, R. E. (1994). Evolution of Interfacial Microstructure between Barium Titanate and Binary Glass. *J. American Ceram. Soc*, Vol. 77, No. 3, pp. 852-856.

Lange, F.F. (1984). Sinterability of Agglomerated Powders. *J. Am. Ceram. Soc.*, Vol. 67, No. 2, pp. 83-89.

Liu, Z.-J. & Shen, Y.G. (2004). Effect of Amorphous Matrix on the Grain Growth Kinetics in Two-Phase Nanostructured Film: A Monte Carlo Study. *Acta Materiala*, Vol. 52, pp. 729-736.

Lo, C.-L. & Duh, J.-G. (2002). Low Temperature Sintering and Microwave Dielectric Properties of Anorthite-Based Glass-Ceramic. *J. Am. Ceram. Soc.*, Vol. 85, No. 9, pp. 2230-2235.

Long, Y., Wang, Y., Wu, W., Wang, D. & Li, Y. (2009). Sintering and Microwave Dielectric Properties of $LiNB_{0.63}Ti_{0.4625}O_3$ Ceramics with the B_2O_3-SiO_2 Liquid Phase Additives. *J. American Ceram. Soc*., Vol. 92, No. 11, pp. 852-856.

Louet, N., Gono, M and Fantozzi, G. (2005). Influence of the Amount of Na_2O and SiO_2 on the Sintering Behavior and the Microstructural Evolution of a Bayer Alumina Powder, *Ceramics International,* Vol. 31, pp. 981-987.

MacLaren, I., Cannon R. M., Gulgun, M. A., Voytovych, R., Nicoletta P.-P.,¶ Scheu, C. Taffner, U. and Ruhle M. (2003). Abnormal Grain Growth in Alumina: Synergistic Effects of Yttria and Silica, *J. Am. Ceram. Soc.,* Vol. 86, No. 4, pp. 650–659.

Matters-Kammerer, M., Mackens, U., Reimann, K., Pietig, R., Hennings, D., Schreinemacher, B., Mauczok, R. , Gruhlke, S. & Martiny, C. (2006). Material Properties and RF Applications of High *k* and Ferrite LTCC Ceramics. *Microelectronics Reliability*, Vol. 46, pp. 134–143.

Muralidhar, S.K., Shaikh, A.S., Robert, G.J., Hankey, D.L., Leandri, D.J. & Vlach, T.J. (1992). *Low Dielectric, Low Temperature Fired Glass-Ceramic*. U.S Patent 5,164,342.

Paik, P.-M., Park, Y.-J, Yoon, M.-S., Lee, J.-H. & Joo, Y.-C. (2003). Anisotropy Grain Boundary Energies as Cause of Abnormal Grain Growth in Electroplated Copper Film. *Scripta Materiala*, Vol. 48, pp. 683-688.

Pampuch, R. (1976). *Ceramic Materials: An Introduction to their Properties.* Elsevier, Scientific Publishing Company, NY.

Pinckney, L. R. and Beall, G.H. (2008). Microstructural Evolution in Some Silicate Glass-Ceramics: A Review. *J. Am. Ceram. Soc.*, Vol. 91, No. 3, pp. 773-779.

Rabe, T., Schiller, W.A., Hochheimer, T., Modes, C. & Kipka, A. (2005). Zero Shrinkage of LTCC Self-Constrained Sintering. *Int. J. Appl. Ceram. Tech.*, Vol. 2, No. 5, pp. 374-382.

Rahaman, M.N. (1995). *Ceramic Processing and Sintering*. Marcel Dekker, Inc. NY.

Raj, P.M. & Cannon, R. (1999). Anisotropy Shrinkage in Tape-Cast Alumina: Role of Processing Parameter and Particle Shape. *J. Am. Ceram. Soc*., Vol. 82, No. 10, pp. 2619-2625.

Rane, S. B., Khanna,.P.K., Seth, T., Phatak, G.J., Amalnerkar, D.P and Das, B.K. (2003). Firing and Processing Effects on Microstructure of Fritted Silver Thick-film Electrode Materials for Solar Cells. *Materials Chemistry and Physics,* Vol. 82, pp. 237-245.

Rohrer, G. S. (2001), The Anisotropic of Metal Oxide Surface Properties; In *Oxide Surfaces,* D.P. Woodruff, pp. 485-513, Elsevier Science, UK.

Sameshima, S., Higashi, K. & Hirata, Y. (2000). Sintering and Grain Growth of Rare-Earth-Doped Ceria Particles. *J. Ceram. Processing*, Vol. 1, No. 1, pp. 27-33.

Sawhill, H.T. (1988). Materials Compatibility and Co-firing Aspect in Low Temperature Co-fired Ceramic Packages. *Ceram. Eng. Sc. Proc.*, Vol. 9, No. 11-12, pp. 1603-1617.

Sergent, J.E. & Harper, C.A. (1995). *Hybrid Microelectronics Handbook*, (2nd Ed.) McGraw-Hills Inc., New York.

Shackelford, J.F. (1992). *Introduction of Materials Science for Engineers*. Macmillan Publishing Company, USA.

Shimada, Y., Utsumi, K., Suzuki, M., Takamizowa, H., Nitta, M. and Watari, T. (1983). Low Firing Temperature Multilayer Glass Ceramic Substrate. *IEEE Trans. Compon. Hybrids Manuf. Tech*., Vol. 6, No. 4, pp. 382-388.

Simpson, Y.K and Carter, B.C. (1990). Faceting Behaviour of Alumina in the Presence of a Glass. *J. Am. Ceram. Soc.,* Vol. 73, No. 8, pp. 2391-2398.

Sone, T.-W,Han, J.-H., Hong, S.-H and Kim, D.-Y .(2001). Effect of Surface Impurities on the Microstructure Development during Sintering of Alumina. *J. Am. Ceram. Soc.*, Vol. 84, pp. 1386-1388.

Tummala, R.R. (1991). Glass-Ceramic Packaging in the 1990's. *J. Am. Ceram. Soc*., Vol. 74, pp. 895-908.

Ubach, R.L.J.M., Schreurs, P.J.G. & Geers, M.G.D. (2004). Microstructure Evolution of Tin-Lead Solder. *IEEE Trans. on Components and Packaging Technologies*, Vol. 27, No. 4, pp. 635-641.

Uematsu, K., Ishaka, S., Shinohara, N. & Okumiya, M. (1997). Grain Oriented Microstructure of Alumina Ceramics Made Through the Injection Moulding Process. *J. Am. Ceram. Soc*., Vol. 80, No. 5, pp. 1313-1315.

Valant, M. & Suvorov, D. (2000). Microstructure vs. Dielectric Property Correlation in the Stoichiometric Sillinites. *Korean J. Crystallography*, Vol. 11, No. 4, pp. 191-194.

Valant, M., Suvorov, D., Pullar, R.C., Sarma, K. & Alford, N. M. (2006). A Mechanism for Low Temperature Sintering. *J. Europ. Ceram. Soc*., Vol. 26, Issue 13, pp. 2777-2783.

Verhoeven, J.D. (1975). *Fundamental of Physical Metallurgy*. John Wiley, New York.

Wang, S.-F., Wang, S.J., Wang, Y.-R., Hsu, Y.-F., Chen, L.-Y. & Tsai, J.-S. (2009). Effect of SiO_2 Addition on the Microstructure and Microwave Dielectric Properties of Ultra Low Fire $Tite_3O_8$ Ceramics. *Ceramics International*, Vol. 35, pp. 1813-1817.

Wang, S.-H and Zhou, H.-P .(2003). Densification and Dielectric Properties of CaO-B_2O_3-SiO_2 System Glass-Ceramics. *Material Science and Engineering B*, Vol. 99, pp. 597-600.

Wang, X. & Atkinson, A. (2011). Microstructure Evolution in Thin Zirconia Films: Experimental Observation and Modeling. *Acta Materialia*, Vol. 59, pp. 2514–2525.

Wu, S.P., Zhao, Q.Y., Zheng, L.Q. and Ding, X. H. (2011). Behaviors of ZnO-doped Silver Thick-Film and Silver Grain Growth Mechanism. *Solid State Science,* Vol. 13, pp. 548-552.

Xiang J.-H., Yong, H. & Xie, Z.-P. (2002). Study of Gel-Tape-Casting Process of Ceramic Materials. *Mat. Sc. & Eng. A,* Vol. 323, Issue 1-2, pp. 336-341.

Yajima, K. & Yamaguchi, T. (1984). Sintering and Microstructure Development of Glass Bonded Silver Thick-Film. *Journals of Material Science*, Vol. 19, pp. 77-84.

Zhou, D., Wang, H., Yao, X. & Phang, L.-X. (2008). Dielectric Behavior and Co-Firing with Silver Monoclinic $BiSbO_4$ Ceramic. *J. Am. Ceram. Soc.*, Vol. 91, No. 4, pp. 1380-1383.

Zhu, H., Liu, M., Zhou, H., Li, L. & Lv, A. (2007). Study on Properties of $CaO\text{-}SiO_2\text{-}B_2O_3$ System Glass-Ceramic. *Materials Research Bulletin*, Vol. 42, Issue 6, pp. 1137-1144.

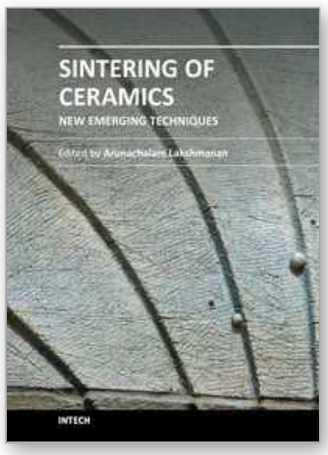

Sintering of Ceramics - New Emerging Techniques
Edited by Dr. Arunachalam Lakshmanan

ISBN 978-953-51-0017-1
Hard cover, 610 pages
Publisher InTech
Published online 02, March, 2012
Published in print edition March, 2012

The chapters covered in this book include emerging new techniques on sintering. Major experts in this field contributed to this book and presented their research. Topics covered in this publication include Spark plasma sintering, Magnetic Pulsed compaction, Low Temperature Co-fired Ceramic technology for the preparation of 3-dimesinal circuits, Microwave sintering of thermistor ceramics, Synthesis of Bio-compatible ceramics, Sintering of Rare Earth Doped Bismuth Titanate Ceramics prepared by Soft Combustion, nanostructured ceramics, alternative solid-state reaction routes yielding densified bulk ceramics and nanopowders, Sintering of intermetallic superconductors such as MgB2, impurity doping in luminescence phosphors synthesized using soft techniques, etc. Other advanced sintering techniques such as radiation thermal sintering for the manufacture of thin film solid oxide fuel cells are also described.

InTech Europe
University Campus STeP Ri
Slavka Krautzeka 83/A
51000 Rijeka, Croatia
Phone: +385 (51) 770 447
Fax: +385 (51) 686 166
www.intechopen.com

InTech China
Unit 405, Office Block, Hotel Equatorial Shanghai
No.65, Yan An Road (West), Shanghai, 200040, China
中国上海市延安西路65号上海国际贵都大饭店办公楼405单元
Phone: +86-21-62489820
Fax: +86-21-62489821

IntechOpen